ABNUS JOURNAL
Your Research Partner

Jurnal Teknika dan Informatika (JTI)
E-ISSN: 2797-0000 | Vol. 6, No. 2 (2026) | pp. 155-175

Summability Methods for Noisy Industrial Reliability Data and Failure Prediction

Avishek Shah[1], Prem Kumar Nayak[2], Suresh Kumar Sahani[3*]

Faculty of Science, Technology, and Engineering, Rajarshi Janak University, Janakpurdham, Nepal[1,2,3]

***Corresponding author:** avishekshah@rju.edu.np | premnayak6511@gmail.com | sureshsahani@rju.edu.np

Received: 19 September 2026 | Revised: 8 October 2026 | Revised: 26 October 2026 | Published: 05 November 2026

Abstract

Purpose: Industrial reliability records contain impulsive noise, drift, missing intervals, maintenance resets, regime changes, and right censored lifetimes, which complicate the estimation of degradation trends and the prediction of failures. This study examines how classical summability ideas, especially Cesàro averaging and Abel type regularization, can be integrated with robust preprocessing, survival analysis, and prognostics.

Research Methodology: The study uses a methodological design that specifies a hybrid workflow of data quality screening, time aware normalization, parallel smoothing at multiple scales, reliability or degradation modeling, blocked temporal validation, uncertainty calibration, and cost aware maintenance decisions, supported by mathematical definitions and generated illustrations.

Results: The illustrations show that short windows leave noise, long windows delay warnings, and the cumulative Cesàro mean recovers only about half of a regime shift after 100 cycles, whereas trailing and Abel type means reach about 90% within 18 cycles. In a pump example, smoothing removed two false alarms at the cost of about two days of warning.

Conclusions: Summability should be treated as a transparent, tunable preprocessing and diagnostic layer rather than as a substitute for a physically meaningful failure model.

Limitations: All numerical illustrations are synthetic, and no empirical performance claim is made.

Contributions. The study maps summability operators to reliability data problems and provides a leakage aware workflow, a comparison protocol, and a decision focused validation checklist.

Keywords: *Abel Summability, Cesàro Mean, Failure Prediction, Industrial Reliability, Survival Analysis*

How to Cite: Shah, A., Nayak, P. K., & Sahani, S. K. (2026). Summability Methods for Noisy Industrial Reliability Data and Failure Prediction. *Jurnal Teknika dan Informatika (JTI)*, 6(2), 155-175.

1. Introduction

Reliability engineering asks whether an asset will perform its required function for a stated period under stated conditions. Industrial monitoring adds a temporal challenge, because measurements arrive continuously, operating conditions vary, and the failure event of interest may be rare or incompletely observed. A bearing vibration signal, pump pressure trace, or motor temperature series can combine gradual degradation with transient disturbances (Lei, Li, Guo, Li, Yan, & Lin, 2018; Zonta, da Costa, de Lima, da Trindade, & Li, 2020). If a model treats every fluctuation as a health change, it may generate nuisance alarms, and if it suppresses too much variation, it may miss a developing fault.

© 2026 Abnus | Open Access — CC BY 4.0 | abnus.co | DOI:10.52909/jti.v6i2.462

Classical reliability analysis offers a disciplined treatment of time to failure, censoring, hazard, and life distributions, while data driven prognostics contributes feature learning and Remaining Useful Life (RUL) prediction (Zonta et al., 2020). Between the raw stream and either modeling family lies a practical question of how unstable, incomplete, or oscillatory measurements should be summarized without erasing the temporal information that signals failure. Summability theory studies transformations of sequences and series, and a summability method may assign a generalized value to a sequence that does not converge in the ordinary sense (Sahani, & Mishra, 2020; Sahani, & Das, 2023). In industrial data processing, related averaging and regularization operators can stabilize estimates over time. The terminology must be used carefully, however, because an ordinary moving average is not a complete summability theory and a smoothed signal is not necessarily a better predictor.

The key research question is therefore not whether smoothing is useful in general, but under what conditions summability improves failure related inference, what information it can destroy, and how its choices should be validated. This question matters because prediction errors have asymmetric costs, since a false alarm causes unnecessary inspection or downtime, while a missed warning causes equipment damage, safety risk, and production loss. The study contributes a precise mapping between summability operators and reliability data problems, a hybrid and leakage aware analytical workflow, a comparison protocol that separates smoothing quality from downstream predictive value, and a decision focused validation checklist. Its numerical illustrations are hypothetical and should be replaced by reproducible tests on a cited or authorized dataset before the framework is described as empirically validated. The proposed workflow is shown in Figure 1.

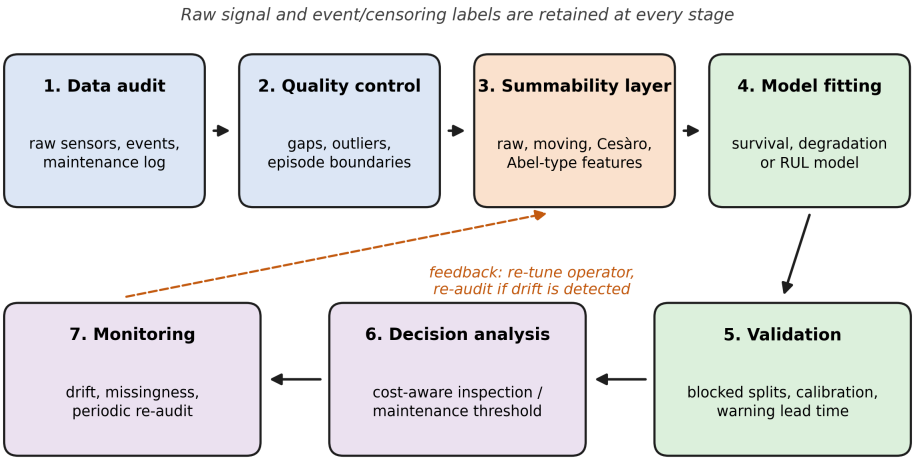


Figure 1. Hybrid summability and reliability workflow

Figure 1 presents the seven stages of the hybrid workflow, namely data audit, quality control, the summability layer, model fitting, validation, decision analysis, and monitoring. The note at the top states that raw signals and event and censoring labels are retained at every stage, which is the central safeguard of the framework because smoothing must never overwrite when or whether a failure occurred. The summability layer computes raw, moving average, Cesàro, and Abel type features in parallel rather than replacing the original signal. The dashed feedback path from monitoring back to the summability layer shows that operators are retuned and the data are re audited whenever drift is detected, so the workflow functions as a closed loop rather than a one time preprocessing step. A typical input to this workflow is illustrated in Figure 2.

© 2026 Abnus | Open Access — CC BY 4.0 | abnus.co | DOI:10.52909/jti.v6i2.462

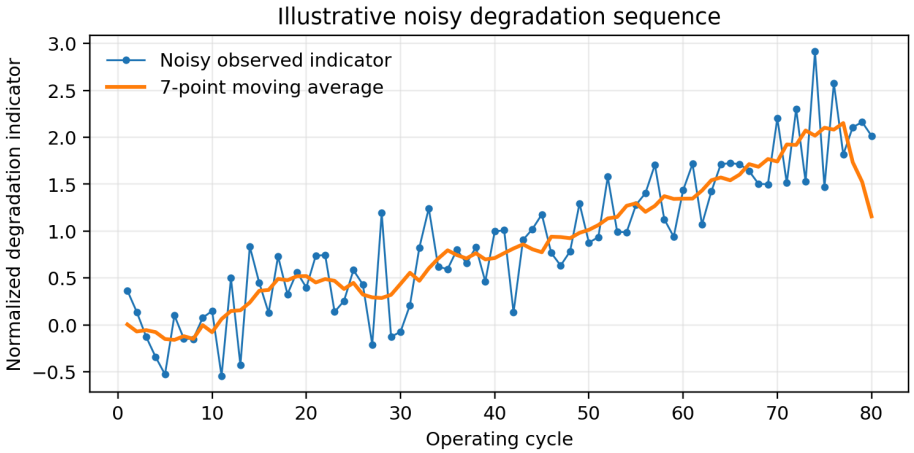


Figure 2. A noisy degradation indicator and a short moving average trend (sequence generated for illustration only)

Figure 2 shows a normalized degradation indicator that rises gradually over 80 operating cycles but is masked by large cycle to cycle fluctuations, together with a seven point moving average. The moving average makes the underlying upward trajectory much easier to see, which illustrates the appeal of smoothing for degradation monitoring. At the same time, the last few points of the moving average bend downward because a finite window has fewer observations at the end of the record, which shows that boundary handling can create artifacts precisely where the most recent and most decision relevant information lies. The figure therefore introduces both the benefit and the main risk that the rest of the study examines.

2. Literature Review and Hypothesis/es Development

2.1 Reliability and Censored Lifetime Data

Reliability analysis begins with a clear event definition and observation scheme. For a nonrepairable unit with lifetime T, reliability is $R(t) = P(T > t)$, the cumulative distribution is $F(t) = 1 - R(t)$, and the hazard $h(t)$ is the instantaneous event rate conditional on survival to t. The exponential model assumes a constant hazard, while the Weibull model allows increasing or decreasing hazard depending on its shape parameter (NIST, 2012). The (NIST, 2012) handbook emphasizes graphical diagnostics, distribution fitting, and maximum likelihood methods for censored data. Right censoring is common in field data because a unit may still be operating at the end of observation. Treating its last observed time as a failure biases lifetime estimates downward, while dropping censored units discards survival information, so the likelihood must include survival contributions for censored observations (Wang, Li, & Reddy, 2019). Machine learning methods for survival analysis extend these principles to high dimensional covariates while keeping censoring explicit (Wang et al., 2019; Syed, Hasan, Chowdhury, Rahman, & Ahmed, 2025).

Industrial equipment is often repaired and returned to service, so a single lifetime distribution may not describe the full process. Maintenance actions can reset some degradation indicators, only partially restore components, or change the operating regime. The data model should therefore distinguish calendar time, operating hours, cycle count, repair episodes, and asset identity. Summability acts on ordered measurements, but the ordering and reset logic must reflect the physical process, and smoothing sensor trajectories must not overwrite event and censoring labels.

2.2 Development of Summability Theory

Sahani and Mishra (2020) studied Nörlund summability of infinite series and its usefulness in examining convergence, Sahani and Mishra (2021) applied Borel's method to Fourier series, and Sahani and Mishra (2020) investigated Cesàro sequence spaces in relation to functional analysis. The

© 2026 Abnus | Open Access — CC BY 4.0 | abnus.co | DOI:10.52909/jti.v6i2.462

approximation of functions using Fourier Laguerre and Legendre series through different summability methods was examined by Sahani and Mishra (2020); Sahani and Mishra (2021), and Sahani and Mishra (2021) studied the approximation of signals using Nörlund summability of derived Fourier series. Further studies investigated decreasing and almost nonincreasing sequences in ultraspherical and double Fourier series (Sahani, Mishra, & Rathour, 2022) and extended these ideas to double, conjugate, and Jacobi series using Nörlund, matrix, and Borel type methods (Sahani et al., 2022; Sahani, Mishra, & Pahari, 2020).

Kushwaha, Thakur, Sahani, and Suryawanshi (2023) examined function approximation through Nörlund summability of double Fourier series, Pokharel, Pahari, and Sahani (2023) investigated almost decreasing sequences associated with Legendre series, and Kushwaha et al. (2023) studied generalized almost matrix summability of Fourier series and their conjugates. Kushwaha et al. (2023) considered the existence and convergence of gamma matrices, Kushwaha et al. (2023) studied convergence rates in absolute summability, and Sahani et al. (2022) explored series transformations and analytic continuation by matrix methods. More recently, Sahani, Sahani, Jha, and Mahato (2026) considered the regularization of divergent series through classical summability methods and highlighted possible applications in reliability and engineering systems. Overall, these studies trace the development of summability theory in function approximation, convergence analysis, and matrix transformations and provide a mathematical foundation for its application to engineering data.

2.3 Prognostics and Predictive Maintenance

Prognostics and Health Management (PHM) estimates current condition and future failure related quantities, including RUL. Public repositories provide well known datasets, including simulated turbofan degradation, bearing measurements, and battery aging records, which support reproducible algorithm development (Lee, Qiu, Yu, Lin, & Rexnord, 2007; Saha, & Goebel, 2007; Saxena, & Goebel, 2008). These datasets are valuable, but their simulated or laboratory origin limits generalization, and a later dataset generated under real flight conditions partly addresses this gap (Arias, Kulkarni, Goebel, & Fink, 2021). Reviews of machinery prognostics identify a persistent gap between laboratory methods and field deployment (Lei, Yang, Jiang, Jia, Li, & Nandi, 2020), and recent reviews describe classifiers, ensemble methods, and sequence models for predictive maintenance while noting evaluation, deployment, and sector specific challenges (Guidotti, Pandolfo, & Pulina, 2025). Deep models can learn nonlinear patterns and estimate RUL from sensor sequences (Zhao, Yan, Chen, Mao, Wang, & Gao, 2019) but require more data and provide less direct explanation than simple statistical baselines. A fair comparison should therefore include transparent baselines, time respecting splits, and metrics aligned with maintenance decisions (Kapoor, & Narayanan, 2023; Sahani, Thakur, & Dubey, 2022).

An important distinction is between anomaly detection, failure classification, survival probability, and RUL regression (Lei et al., 2020). A model that detects a deviation is not automatically calibrated to estimate failure probability, and a low RUL error on run to failure trajectories does not establish a reliable false alarm rate in a fleet where most units have not failed. Rare failures also create class imbalance that distorts accuracy based evaluation (Haixiang, Yijing, Shang, Mingyun, Yuanyue, & Bing, 2017), and anomaly detection methods are often needed where failure labels are scarce (Pang, Shen, Cao, & van den Hengel, 2022). The proposed hybrid approach preserves these distinctions.

2.4 Smoothing, Robust Statistics, and Change Points

Moving averages and exponential smoothing reduce high frequency variation, but their effects depend on window length, sampling frequency, and the signal's temporal structure. Median filters can resist isolated spikes, and robust scale estimators can limit the influence of outliers. However, filtering is not neutral, because a long window attenuates short lived peaks and shifts the apparent onset of a change, and in failure prediction that delay can matter more than a modest reduction in residual variance. Change point methods target abrupt distributional changes rather than assuming that all variation is noise (Truong et al., 2020). A regime shift may represent a fault, a load change, a sensor replacement,

or an intervention, and models trained before such a shift may degrade under concept drift (Lu et al., 2019). Smoothing should therefore be paired with raw signal monitoring and change point checks rather than applied as an irreversible cleaning step.

2.5 Summability Concepts and the Research Gap

The Cesàro method replaces a sequence by running averages of its terms. For a sequence x_n, the first order Cesàro mean is $\sigma_n = (x_1 + \ldots + x_n)/n$. If x_n converges to L, then σ_n also converges to L, but the converse does not hold in general, since $x_n = (-1)^n$ diverges while σ_n tends to 0. Abel type methods use power weighted sums, commonly expressed through a parameter r approaching one from below. Such operators provide a principled language for controlled averaging, but their classical purpose is not identical to industrial denoising. The gap addressed here is methodological rather than a claim that summability is a newly discovered reliability tool. Reliability and PHM research has strong methods for censored survival data and data driven prediction, while summability theory supplies operators with interpretable averaging behavior, but few workflows explicitly test summability choices against censoring, regime shifts, calibration, and maintenance costs. The main method families are compared in Table 1.

Table 1. Conceptual comparison of method families

Method Family	Primary Target	Strength	Important Risk
Reliability and survival models	Failure time distribution	Handles censoring and gives interpretable survival quantities	Distributional assumptions may be restrictive
Moving and exponential averages	Short term signal stability	Simple, inexpensive, and transparent	Lag and peak attenuation
Robust filters	Spikes and outliers	Less sensitive to isolated extremes	Can suppress true impulsive faults
Machine learning prognostics	Classification or RUL	Captures nonlinear multivariate patterns	Data demand, drift, calibration, and leakage
Summability operators	Sequence regularization and averaging	Formal parameterized averaging framework	Operator choice does not guarantee better prediction

Table 1 compares five method families by their primary target, main strength, and most important risk. Reliability and survival models handle censoring explicitly but rely on distributional assumptions, moving averages and robust filters are simple and transparent but can attenuate or suppress genuine fault signatures, and machine learning prognostics captures complex patterns at the cost of data demand, drift, and leakage risks (Kapoor & Narayanan, 2023). Summability operators add a formal and parameterized vocabulary for averaging, but the last column stresses that choosing an operator does not by itself guarantee better prediction. The table therefore shows that the families are complementary, which motivates a hybrid design in which summability supplies candidate features that are then judged by the downstream reliability or prognostic model.

3. Research Methodology

3.1 Study Design

This study is a methodological synthesis that specifies an analytical framework, defines its operators and models mathematically, and interprets generated illustrations. No real plant dataset was analyzed, no model was fitted to National Aeronautics and Space Administration (NASA) records, and no numeric result should be cited as an empirical finding. The illustrations are designed to explain expected behaviors and trade offs and to provide a protocol for future experiments.

3.2 Problem Formulation and Summability Operators

Let $x_{i,t}$ denote a sensor derived feature for asset i at operating time t, and let $z_{i,t}$ contain operating context such as load, speed, ambient temperature, or production mode. Let T_i be the observed event or censoring time, with δ_i=1 if failure is observed and δ_i=0 otherwise. A valid pipeline retains raw x, processed features, timestamps, intervention records, and the censoring indicator separately, because smoothing changes the feature representation but must never change whether or when failure occurred. For an ordered sequence x_1, …, x_n, the first order Cesàro mean is given in Formula 1.

$$\sigma_n = \frac{1}{n}\sum_{k=1}^{n} x_k \tag{1}$$

This cumulative form stabilizes a running estimate but assigns substantial weight to old observations. A finite window mean of width w is given in Formula 2.

$$m_t^{(w)} = \frac{1}{w}\sum_{j=0}^{w-1} x_{t-j} \tag{2}$$

A weighted exponential average is defineFormula 3d recursively in Formula 3, where $0 < \alpha \leq 1$.

$$s_t = \alpha x_t + (1-\alpha)\, s_{t-1} \tag{3}$$

In an Abel type transform, a power paramFormula 4eter $0 < r < 1$ weights an observation that is j steps old by r^j, and a normalized finite form is given in Formula 4.

$$A_n(r) = \frac{\sum_{j=0}^{n} r^j x_{n-j}}{\sum_{j=0}^{n} r^j} \tag{4}$$

This expression approaches the cumulative mean as r tends to 1 and is used here as a practical weighted regularizer, not as a claim that all classical Abel summability definitions are identical. More generally, any causal weighted feature can be written as a sum of past observations with nonnegative weights that sum to one, which makes the memory profile of each operator explicit. The symbols used in the framework are summarized in Table 2.

Table 2. Symbols and their operational meanings

Symbol	Definition	Role
$x_{i,t}$	Observed feature for asset i at time t	Noisy input
$z_{i,t}$	Operating context or covariates	Regime adjustment
T_i	Failure or censoring time	Survival endpoint
δ_i	1 for observed failure and 0 for censored	Likelihood indicator
$R(t)$	$P(T > t)$	Reliability function
$h(t)$	Conditional instantaneous failure rate	Risk over time
σ_n	Cumulative Cesàro mean	Running stabilization
$m_t^{(w)}$	Trailing moving average of width w	Finite memory smoothing

© 2026 Abnus | Open Access — CC BY 4.0 | abnus.co | DOI:10.52909/jti.v6i2.462

Symbol	Definition	Role
$A_n(r)$	Normalized Abel type weighted mean	Tunable recency weighting
$\hat{T}$ or RÛL	Predicted event time or remaining useful life	Prognostic output

Table 2 defines ten symbols and links each to its role in the workflow. The first four symbols describe the data, namely the noisy input feature, the operating context used for regime adjustment, the failure or censoring time, and the censoring indicator that enters the likelihood. The next two describe reliability quantities, and the following three describe the summability operators, each with a different memory structure, namely cumulative stabilization for the Cesàro mean, finite memory for the trailing average, and tunable recency for the Abel type mean. The final symbol represents the prognostic output. Keeping these quantities notationally distinct reinforces the principle that smoothed features are inputs to a model and not reliability probabilities themselves.

3.3 Data Quality and Segmentation

Before applying an operator, the analyst should verify timestamp monotonicity, duplicate records, unit consistency, sensor saturation, and missingness. Gaps should not be filled across long outages without a documented model, and resampling is appropriate only when the sampling grid and aggregation rule are meaningful. Sensor features should be normalized using training period statistics only, because full series normalization leaks future information into earlier predictions (Kapoor & Narayanan, 2023). Segmentation should reflect physical continuity, because a maintenance overhaul may create a new episode, a sensor replacement may create a measurement discontinuity, and a load change may alter the signal distribution without indicating damage. A smoothing window must not cross an episode boundary unless a domain expert has justified that continuity assumption. The behavior of the cumulative Cesàro mean on an irregular sequence is shown in Figure 3.

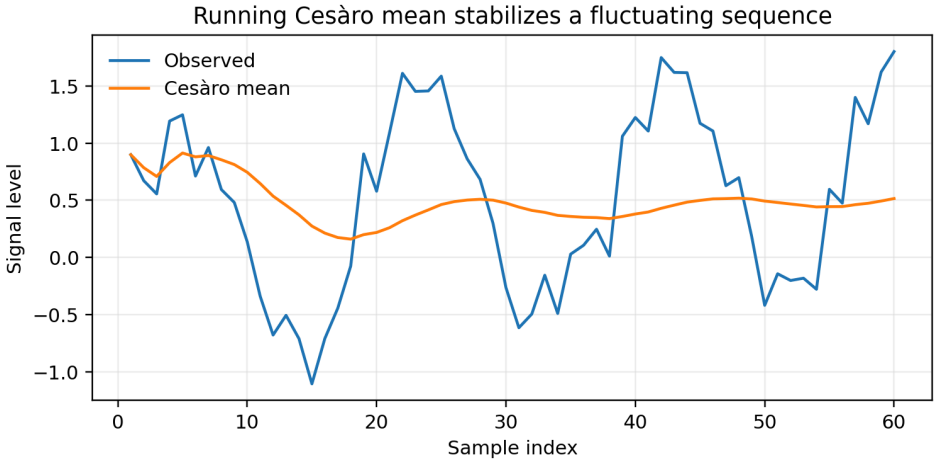


Figure 3. Running Cesàro mean applied to a fluctuating synthetic sequence

Figure 3 shows a synthetic signal that oscillates strongly between about −1.1 and 1.8 over 60 samples, together with its running Cesàro mean. The Cesàro mean quickly settles into a narrow band around 0.3 to 0.5 and remains there despite large swings in the observed values, which illustrates the stabilizing property that makes cumulative averaging attractive for summarizing irregular sequences. However, the same figure reveals its long memory, because the mean barely responds to the sustained rise at the end of the record. The figure therefore demonstrates qualitative stabilization but does not prove improved failure prediction, which requires fitting the same downstream model to each representation and evaluating predictions on future observations.

3.4 Candidate Operators and Parameter Selection

A practical design evaluates at least four candidates, namely no smoothing, a short trailing mean, the cumulative Cesàro mean, and a recency weighted Abel type mean, with a median filter added where

© 2026 Abnus | Open Access — CC BY 4.0 | abnus.co | DOI:10.52909/jti.v6i2.462

impulsive contamination is credible. The objective is not to select the visually smoothest series but to choose a representation that improves out of sample reliability estimates while preserving early warning information. Smoothing parameters should be selected within training and validation periods using blocked time splits, and assets rather than individual rows should be separated when cross asset generalization is the goal. For online deployment, the transform must be causal, so centered moving averages are unsuitable for real time prediction. The sensitivity to window length is shown in Figure 4.

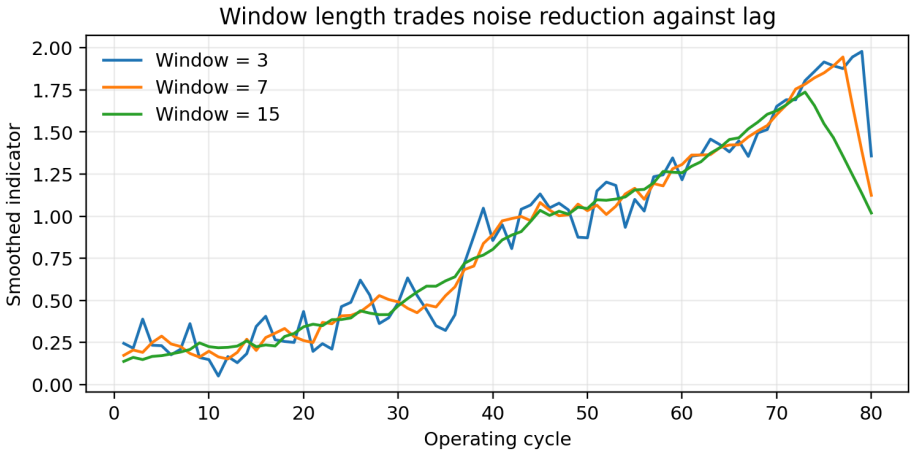


Figure 4. Window length sensitivity, showing that wider windows smooth more but may delay a trend change

Figure 4 compares moving averages with windows of 3, 7, and 15 cycles applied to the same rising degradation indicator. The three point window follows the signal closely and retains much of its noise, the seven point window gives a cleaner trend, and the fifteen point window is the smoothest but reacts more slowly to the acceleration after about cycle 40. All three curves drop sharply at the end of the record because of edge effects, with the widest window affected most. The figure illustrates that wider windows suppress high frequency variation at the price of delayed response, which is a structural property of averaging rather than a defect that tuning can remove, so the raw signal and change point features should remain available alongside the smoothed trend (Truong et al., 2020).

3.5 Reliability and Prognostic Models

For a continuous lifetime T with density $f(t)$, distribution $F(t)$, and survival $R(t) = 1 - F(t)$, the hazard is $h(t) = f(t)/R(t)$, and the cumulative hazard $H(t)$ satisfies $R(t) = \exp[-H(t)]$. Under a Weibull model with shape $k > 0$ and scale $\lambda > 0$, the reliability and hazard functions are given in Formula 5.

$$R(t) = exp\left[-\left(\frac{t}{\lambda}\right)^{k}\right], \qquad h(t) = \frac{k}{\lambda}\left(\frac{t}{\lambda}\right)^{k-1} \tag{5}$$

For independent observations with event indicator δ_i, the log likelihood combines failure density contributions for observed failures and survival contributions for censored units, as shown in Formula 6.

$$\ell = \sum_{i} \{\delta_i log f(T_i) + (1 - \delta_i) log R(T_i)\} \tag{6}$$

This formulation makes clear why censored records contribute survival information rather than being discarded or mislabeled as failures (Wang et al., 2019). For degradation based prediction, a model may estimate a latent health indicator or RUL, which should be evaluated on held out future periods or assets with a documented target construction, because RUL labels in run to failure datasets are computed from the final cycle while in field data the true failure horizon is often unknown. An illustrative Weibull reliability curve is shown in Figure 5.

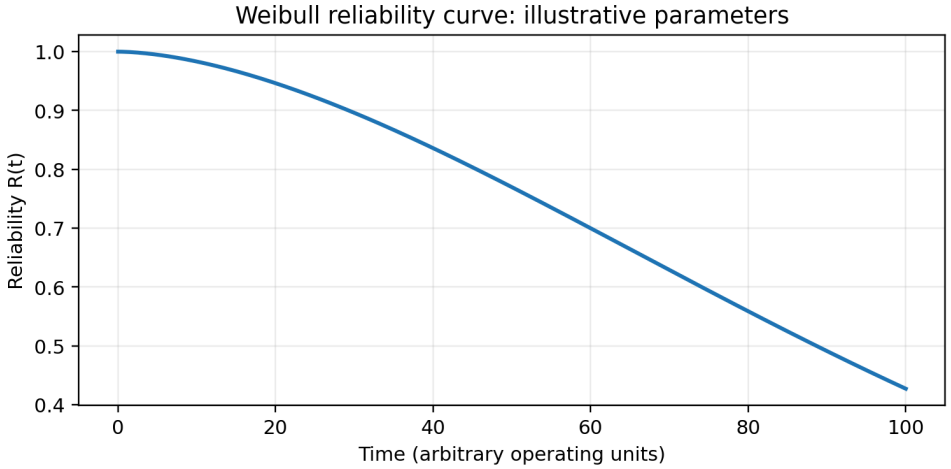


Figure 5. Illustrative Weibull reliability curve (parameters chosen for explanation, not fitted to plant data)

Figure 5 shows a Weibull reliability function that declines slowly from 1.0 at time zero and then more steeply, reaching about 0.43 at 100 operating units. The concave early shape followed by a steeper decline reflects a shape parameter greater than one, which corresponds to an increasing hazard typical of wear out failures in mechanical components. The figure illustrates the model form that a survival analysis would fit to failure and censoring times, while the smoothed sensor features of Section 3.2 serve as covariates or health indicators. The parameters are chosen only for explanation, so the curve should not be interpreted as a fitted lifetime law for any industrial population.

3.6 Hybrid Workflow and Operational Algorithm

The workflow proceeds in seven stages. The data audit retains raw observations and creates a data dictionary, asset identifier, event definition, censoring status, maintenance history, and operating context, and quality control flags gaps, outliers, sensor faults, and episode boundaries. The parallel representation stage computes raw and candidate smoothed features and records the operator and parameter for every derived column. Model fitting estimates a reliability model, a degradation model, or both, validation uses chronological splits and asset level holdouts with calibration and early warning metrics, decision analysis translates predictions into thresholds using the relative costs of false alarms, missed failures, and downtime, and monitoring detects distribution drift and periodically re evaluates the pipeline (Lu et al., 2019). The framework is modular, so summability can be removed if it fails to improve a baseline, and a complex model can be replaced by a Weibull or proportional hazards model when data are sparse. The corresponding operational algorithm is shown in Figure 6.

© 2026 Abnus | Open Access — CC BY 4.0 | abnus.co | DOI:10.52909/jti.v6i2.462

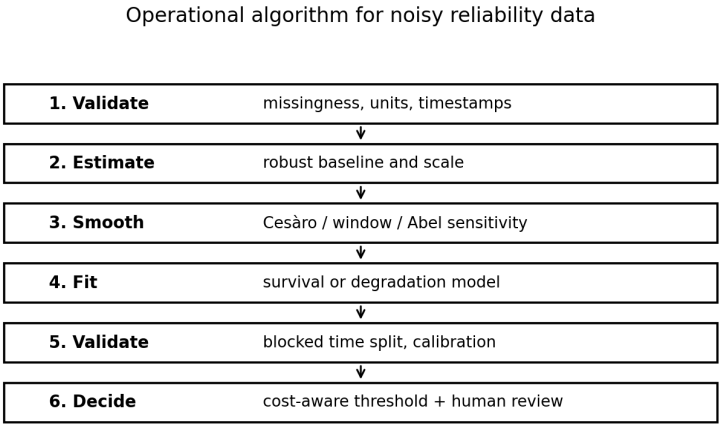


Figure 6. Operational algorithm for applying summability without losing event metadata

Figure 6 presents the operational algorithm as six sequential steps, namely validating missingness, units, and timestamps, estimating a robust baseline and scale, smoothing with Cesàro, window, and Abel sensitivity, fitting a survival or degradation model, validating with blocked time splits and calibration, and deciding with a cost aware threshold and human review. In practice, these steps also require segmenting sequences at documented resets, fitting normalization and imputation rules on training data only, tuning operator parameters within blocked validation folds, and reporting all settings, uncertainty, failure cases, and monitoring triggers. The figure shows that smoothing is only the third of six steps and is bracketed by validation before and after it, which reinforces that the operator is a tested candidate rather than an unquestioned preprocessing default.

3.7 Evaluation Protocol and Reproducibility

Signal level diagnostics include residual scale, lag around known changes, and stability across operating regimes, while prediction metrics depend on the task. For RUL regression, the Mean Absolute Error (MAE) and Root Mean Squared Error (RMSE) are common and are defined in Formula 7, although they do not encode the asymmetric cost of early versus late predictions.

$$MAE = \frac{1}{n}\sum_{i=1}^{n}\left|y_i - \hat{y}_i\right|, \qquad RMSE = \sqrt{\frac{1}{n}\sum_{i=1}^{n}\left(y_i - \hat{y}_i\right)^2} \tag{7}$$

For failure classification, precision recall curves are more informative than accuracy under severe class imbalance (Haixiang et al., 2017), and for survival prediction, time dependent discrimination and calibration diagnostics should be used because a concordance statistic alone does not establish calibrated probabilities (Wang et al., 2019). Confidence intervals should account for clustering by asset, and hyperparameters must be chosen without using the final test set. The recommended measures are summarized in Table 3.

Table 3. Recommended evaluation measures

Task	Measure	Question Answered	Caution
Signal smoothing	Residual scale and step response lag	Did noise fall and how much delay was introduced	Lower variance alone may hide a fault
RUL regression	MAE, RMSE, and error by horizon	How far are predictions from the reference RUL	Reference RUL may be simulation derived
Failure classification	Precision, recall, and PR AUC	How well are rare failures detected	Threshold and class prevalence matter

© 2026 Abnus | Open Access — CC BY 4.0 | abnus.co | DOI:10.52909/jti.v6i2.462

Task	Measure	Question Answered	Caution
Survival modeling	Calibration, time dependent AUC, and concordance	Are risk rankings and probabilities credible	Concordance does not ensure calibration
Maintenance policy	Expected cost, downtime, and missed event rate	Does the decision improve operations	Costs must be locally estimated

Table 3 matches each analytical task with its appropriate measures, the question they answer, and a caution about their interpretation. Signal level smoothing should be judged by both residual reduction and step response lag, because lower variance alone may hide a fault. RUL regression uses MAE and RMSE, ideally reported by horizon, failure classification uses precision, recall, and the Precision Recall Sarea under the Curve (PR AUC), and survival modeling uses calibration and time dependent discrimination. The last row connects all these measures to the maintenance policy through expected cost, downtime, and missed event rate, which must be estimated locally. Each experiment should also record the data version, split definition, random seed, feature transformations, model settings, censoring rules, and software versions, with every smoothed representation using the same split and downstream model as the raw baseline so that any gain can be attributed to summability rather than to model capacity or leakage (Kapoor & Narayanan, 2023).

4. Results and Discussions

4.1 Noise Reduction and Trend Lag

The illustrations in Figures 2 and 4 show that a short average makes an underlying trajectory easier to see, but that the first and last points of a finite sequence are affected by boundary handling and that wider windows react more slowly to change. A production implementation should therefore document edge handling or use a causal filter. The overall trade off between noise reduction and lag is summarized schematically in Figure 7.

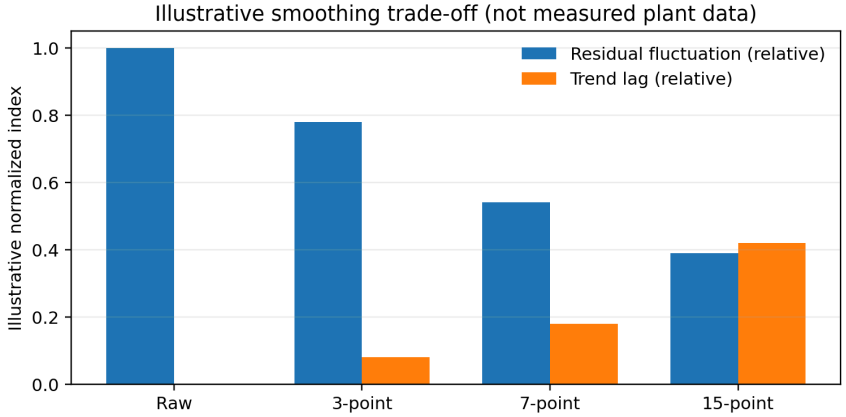


Figure 7. Illustrative normalized comparison of noise reduction and trend lag (values are schematic, not measured)

Figure 7 compares the raw signal with three point, seven point, and fifteen point averages on two normalized indices, namely residual fluctuation and trend lag. Residual fluctuation falls from 1.0 for the raw signal to about 0.78, 0.54, and 0.39 as the window widens, while trend lag rises from zero to about 0.08, 0.18, and 0.42. The two curves cross between the seven point and fifteen point windows, which illustrates that beyond a certain width, additional smoothing buys little noise reduction at a large cost in delay. The figure communicates the multiobjective nature of operator selection, in which a useful sensitivity analysis plots performance against window width together with lag and calibration, and if several nearby settings perform similarly, selection can prioritize interpretability. The values are schematic and not measured.

© 2026 Abnus | Open Access — CC BY 4.0 | abnus.co | DOI:10.52909/jti.v6i2.462

4.2 Comparing Smoothing Families

The cumulative Cesàro mean suits a running average when the process is stable or slowly changing, but its long memory means that old values continue to influence the estimate and a regime change may be diluted for a long period. A finite window average forgets old observations after w samples, making it more responsive but sensitive to the chosen window, while an Abel type weighted average provides a parameterized recency profile whose benefits depend on normalization and parameter selection. This memory effect is made concrete with a synthetic regime shift in Figure 8.



Figure 8. Synthetic step response comparison after an abrupt regime shift at cycle 100, showing (a) cumulative Cesàro, trailing mean (w = 20), and Abel type (r = 0.9) estimates and (b) RMSE to the true level before and after the shift (generated values, not industrial data)

Figure 8 shows in panel (*a*) that after the true level jumps from 1.0 to about 2.2 at cycle 100, the cumulative Cesàro mean, which weights all past samples equally, recovers only about half of the step after 100 more cycles, whereas the trailing mean and the Abel type weighted mean reach about 90% of the new level within roughly 18 cycles. Panel (*b*) shows the price of that responsiveness, because before the shift the Cesàro mean has the lowest tracking error, while after the shift its RMSE rises to about 0.84 compared with about 0.30 for the trailing mean and 0.25 for the Abel type mean. The figure therefore demonstrates that a shorter memory averages fewer samples and is noisier in stable periods, but adapts much faster to change. The exact lags depend on the window, decay parameter, and noise level. How a benchmark might report the downstream effect of these operators is shown in Figure 9.

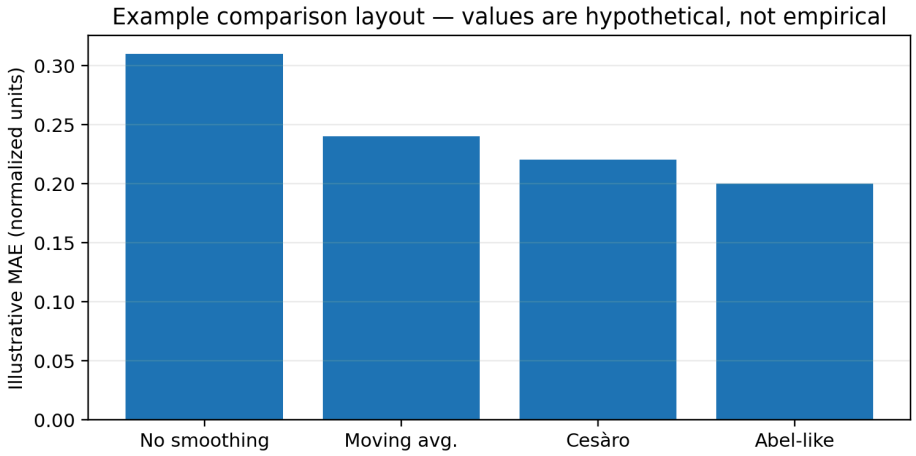


Figure 9. Hypothetical comparison chart showing how a benchmark table might report MAE (values are not empirical)

Figure 9 shows a hypothetical layout in which the MAE of an RUL model falls from about 0.31 with no smoothing to 0.24 with a moving average, 0.22 with the Cesàro mean, and 0.20 with an Abel type mean. The chart is included only to show how results should be reported once a real experiment has been run, with every representation evaluated by the same downstream model and split. The values are explicitly hypothetical, and the figure should not be read as evidence that summability improves prediction, because a smoothing operator may reduce signal level noise yet worsen RUL prediction if it attenuates an early fault precursor or shifts its onset.

4.3 Reliability Interpretation

Smoothing sensor features and fitting a lifetime distribution address different parts of the problem. Smoothing operates on covariate measurements, while survival analysis represents the event time distribution and censoring mechanism, and conflating the two can lead to invalid conclusions, since a smoother health index cannot correct informative censoring or a misspecified event definition. The complementarity of reliability and cumulative failure probability is shown in Figure 10.

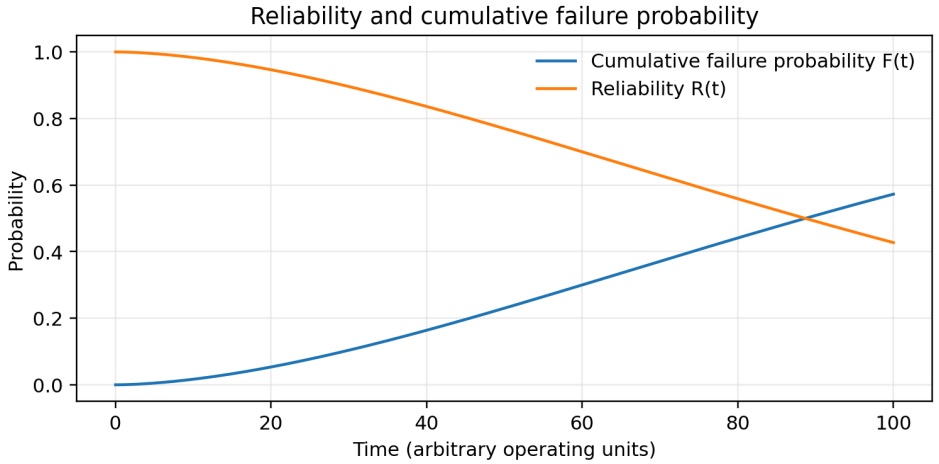


Figure 10. Reliability and cumulative failure probability for the same illustrative Weibull model

Figure 10 plots the reliability $R(t)$ and the cumulative failure probability $F(t)$ for the Weibull model of Figure 5. The two curves are mirror images that always sum to one, crossing at about 0.5 near 90 operating units, where half of the population is expected to have failed. Because $F(t) = 1 - R(t)$, these are not independent metrics, and reporting both adds no new information. A calibrated survival model should produce probabilities that correspond to observed event frequencies over the relevant horizon, and the figure is an illustration of the model form rather than a fitted lifetime law for a specific industrial population.

4.4 Results Template

To keep reporting honest, a structured template for a future experiment is provided instead of invented empirical scores. Values should be filled only after the protocol has been executed on an identified dataset, and the same principle applies to any claim about the percentage improvement in false alarms, maintenance cost, or RUL error. The template is presented in Table 4.

Table 4. Results template to populate after a reproducible experiment

Representation	MAE (RUL)	PR AUC	Calibration Error	Warning Lead Time	95% Interval
Raw features	Report measured value	Report measured value	Report measured value	Report measured value	Report measured interval
Short moving average	Report measured value	Report measured value	Report measured value	Report measured value	Report measured interval
Cesàro mean	Report measured value	Report measured value	Report measured value	Report measured value	Report measured interval

Representation	MAE (RUL)	PR AUC	Calibration Error	Warning Lead Time	95% Interval
Abel type weighted mean	Report measured value	Report measured value	Report measured value	Report measured value	Report measured interval

Table 4 lists four representations, namely raw features, a short moving average, the Cesàro mean, and the Abel type weighted mean, and five outcome measures that should be reported for each, namely MAE for RUL, PR AUC, calibration error, warning lead time, and a 95% interval. Every cell deliberately reads report measured value, because the purpose of the table is to fix the reporting structure before any experiment is run and thereby prevent selective reporting. Combining signal level, predictive, calibration, and operational measures in one table ensures that a representation cannot be declared superior on the basis of a single favorable metric.

4.5 Prediction Error and Uncertainty

Diagnostic plots help reveal systematic bias in RUL predictions. A synthetic example of predicted against reference RUL is shown in Figure 11.

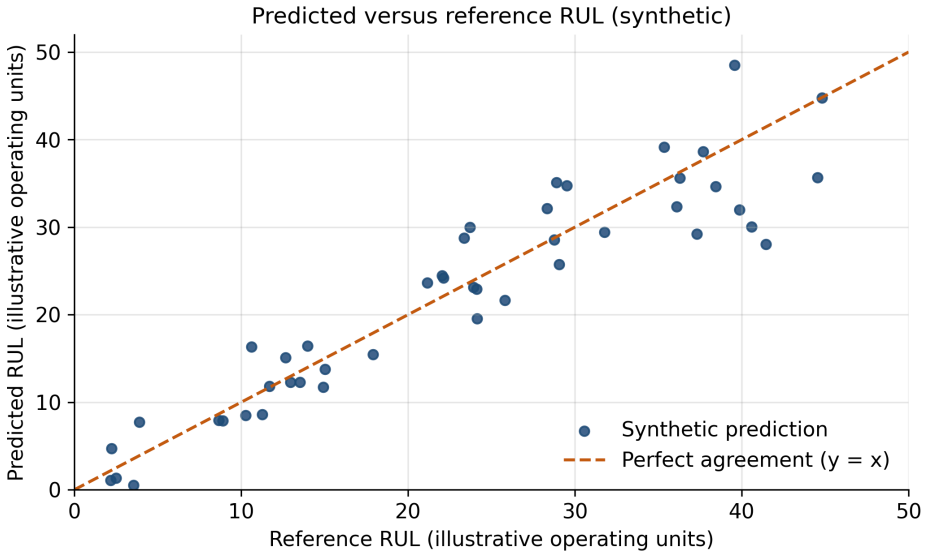


Figure 11. Synthetic predicted versus reference RUL plot (generated values, not observed industrial data)

Figure 11 plots synthetic predicted RUL against reference RUL, with the dashed identity line representing perfect agreement. Points close to the line at low RUL indicate accurate predictions near failure, while the wider scatter at higher RUL, including predictions that overestimate by more than ten units, shows that uncertainty typically grows with the prediction horizon. The plot clarifies a diagnostic rather than reporting model performance, and in a real experiment points should be colored or faceted by asset, operating regime, and horizon to reveal systematic bias. A reliable system should communicate uncertainty rather than a single RUL value, using bootstrap, Bayesian, or quantile intervals whose coverage is validated, because intervals may widen when signals depart from training conditions or failure modes change.

4.6 Fair Comparison of Methods

A fair comparison begins with one locked split and identical target definitions. The raw, moving average, Cesàro, and Abel type pipelines should share the same covariates, downstream model family, hyperparameter budget, and stopping rule, with smoothing parameters selected inside training folds. Results should be reported as a distribution across folds or assets, and an acceptable warning window should be defined in advance, because a prediction that arrives after the maintenance lead time may be statistically close yet operationally useless. If the target is failure within horizon τ, censored cases

© 2026 Abnus | Open Access — CC BY 4.0 | abnus.co | DOI:10.52909/jti.v6i2.462

before τ must be handled with a survival aware method rather than labeled as nonfailures. The required design practices are summarized in Table 5.

Table 5. Failure prediction comparison checklist

Design Item	Required Practice	Reason
Temporal split	Train on earlier periods and test on later periods	Prevents future leakage
Asset split	Hold out assets when generalizing to new units	Tests cross unit transfer
Censoring	Use survival aware labels and likelihoods	Avoids false nonfailure labels
Parameter selection	Tune smoothing only within training folds	Limits optimistic bias
Baselines	Include raw and simple statistical models	Tests whether complexity is justified
Uncertainty	Report intervals and calibration	Supports safe decision making
Operational utility	Specify lead time and cost thresholds	Connects scores to maintenance

Table 5 lists seven design items that a valid comparison must satisfy, each with its required practice and rationale. Temporal and asset splits prevent future leakage and test transfer to new units, survival aware labels avoid treating censored units as nonfailures, and tuning smoothing only within training folds limits optimistic bias (Kapoor & Narayanan, 2023). Including raw and simple statistical baselines tests whether complexity is justified, reporting intervals and calibration supports safe decisions, and specifying lead time and cost thresholds connects statistical scores to maintenance value. The checklist therefore operationalizes the principle that any apparent gain from summability must survive the same rigorous conditions as the baseline.

4.7 From Statistical Performance to Maintenance Value

Maintenance policy is an optimization problem under uncertainty. Let C_{FP} be the cost of a false alarm, C_P the cost of a missed failure, and C_I the cost of inspection or planned intervention. A simple expected cost policy compares the predicted failure probability over horizon τ with a threshold derived from these costs, although in practice the cost structure also includes lost production, spare part lead time, safety consequences, and downtime caused by inspection. The threshold should not be chosen solely to maximize the F1 score, because a high recall threshold may suit a catastrophic failure mode while an inexpensive, easily replaced component may justify a different policy. The decision variables are summarized in Table 6.

@tabledefines six variables that turn a calibrated prediction into a maintenance action. The three cost variables capture the consequences of false alarms, missed failures, and planned interventions, the horizon τ reflects the lead time needed to prepare an intervention, and the predicted failure probability must come from a calibrated model. The threshold is then chosen to minimize expected cost under operational constraints. The estimation column emphasizes that costs are plant specific and should be estimated with operations, maintenance, and safety stakeholders and accompanied by sensitivity ranges rather than a single unqualified optimum.

4.8 Alternatives and Deployment Governance

A median filter may outperform a mean when isolated spikes are sensor artifacts but may erase true impulsive signatures, a Kalman filter is attractive when a state space model is defensible, Gaussian processes provide uncertainty but may scale poorly, and deep temporal models learn complex dependencies but demand careful splitting and calibration (Serradilla et al., 2022). The summability layer is best viewed as a low complexity candidate in this toolkit, and for small fleets classical reliability models and expert features may be more credible than high capacity networks. Simple operators are also easier to explain to maintenance engineers, because a window or decay parameter

can be related to sample rate and degradation time scale, although a cumulative mean can be hard to interpret after a repair reset and a visually smooth curve can create false confidence. Lightweight operators also suit edge devices with limited computing resources (Njor et al., 2024). Deployment should include human review, explicit alarm thresholds, and records of how recommendations were acted upon, because model influenced inspections create selectively observed data that can bias later training. The deployment checks are summarized in Table 7.

Table 7. Deployment checklist for an auditable pipeline

Phase	Check	Evidence to Retain
Data intake	Units, timestamps, IDs, and event definition verified	Data dictionary and validation report
Preprocessing	No future leakage and episode boundaries respected	Transformation specification
Summability	Operator, parameter, and edge handling documented	Versioned configuration
Modeling	Censoring and competing risks addressed	Model assumptions and diagnostics
Validation	Time and asset splits locked and calibration checked	Fold level metrics and intervals
Decision	Lead time and cost threshold agreed	Policy rationale and sensitivity analysis
Monitoring	Drift, missingness, and false alarms reviewed	Periodic audit and incident log

Table 7 organizes deployment into seven phases, from data intake to monitoring, each with a specific check and the evidence that must be retained. The summability phase requires the operator, parameter, and edge handling to be documented in a versioned configuration, so that any alarm can be traced back to the exact transformation that produced it. Validation requires locked time and asset splits with calibration checks, the decision phase requires an agreed lead time and cost threshold with sensitivity analysis, and monitoring requires periodic audits of drift, missingness, and false alarms (Lu et al., 2019). A publishable study should additionally report dataset sources and licenses, sampling cadence, failure definition, censoring rate, and the exact prediction horizon, and it should report negative findings, since a representation that improves visual stability but not prediction is also useful evidence.

4.9 Applications and a Worked Example

The framework targets assets that are monitored continuously, fail rarely, and are expensive to stop. Five such settings are summarized in Table 8, with the data problem each one brings, the operator to test first, and the main caution.

Table 8. Application scenarios for summability based preprocessing

Application	Typical Signals and Data Problems	First Operator to Test	Key Caution
Pumps, motors, and fans in process plants	Bearing vibration and casing temperature with impulsive spikes, load dependent levels, and maintenance resets	Median prefilter, then a trailing or Abel type mean	Do not average across a repair or load change and keep the raw signal
Hydropower turbine and generator units	Bearing temperature and shaft vibration with seasonal flow changes and frequent start and stop cycles	Abel type mean within each operating regime	Segment by regime so that a seasonal shift is not read as damage
Wind turbine gearboxes and generators	SCADA temperatures and power depending on wind speed and ambient temperature	Trailing mean of context adjusted residuals	Adjust for operating context first

Application	Typical Signals and Data Problems	First Operator to Test	Key Caution
Lithium ion battery packs	Capacity or internal resistance per cycle with slow fade, temporary recoveries, and scatter	Cesàro mean for long term fade and a short window for recent change	Cumulative averaging lags behind an accelerating fade
Turbofan engines (benchmark data)	Multisensor health channels under several operating conditions	Channel wise trailing or Abel type features ahead of an RUL model	Simulated degradation may not transfer to fielded engines

Table 8 shows that the appropriate operator depends on how each type of signal ages and what disturbs it. For pumps, motors, and fans, impulsive spikes call for a median prefilter followed by a trailing or Abel type mean, while hydropower and wind applications require segmentation or adjustment for operating context before any averaging. For battery packs, the slow capacity fade measured in records such as those of Saha and Goebel (2007) and studied by Severson et al. (2019) suits a Cesàro mean, but cumulative averaging lags behind accelerating fade, and for turbofan benchmarks (Saxena & Goebel, 2008) channel wise features should feed an RUL model with the caution that simulated degradation may not transfer. The entries are starting hypotheses to be tested under the protocol of Section 3, not results obtained in those industries.

A small worked example shows how the pieces fit together. Consider a hypothetical centrifugal pump whose bearing vibration is logged once a day as velocity RMS in mm/s. In normal operation the readings sit near 2 mm/s, on two days a neighboring machine is started and the reading jumps briefly, and from day 80 a bearing defect begins to grow. An alarm limit of 3.0 mm/s and a failure limit of 7.0 mm/s are assumed, a false alarm is any day before day 80 on which the signal exceeds the alarm limit, and a true warning is the first day after day 80 from which the signal stays above the limit for three consecutive days. The readings, limits, and outcomes are generated for this study and are not plant measurements. The results are shown in Figure 12.

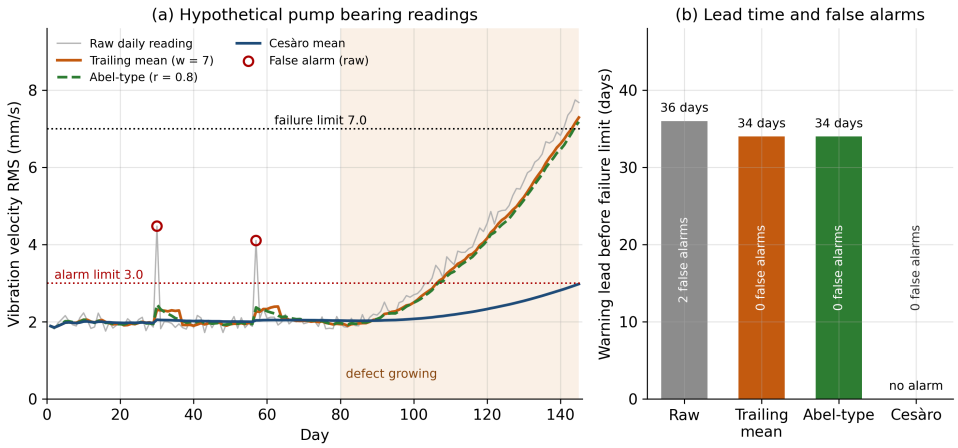


Figure 12. Hypothetical worked example of pump bearing monitoring, showing (a) daily vibration readings with trailing, Abel type, and Cesàro estimates against assumed alarm and failure limits and (b) warning lead time before the failure limit and number of false alarms (generated values, not plant data)

Figure 12 shows in panel (*a*) that the raw readings cross the alarm limit on both startup days, giving two false alarms, whereas the trailing mean (w=7) and the Abel type mean (r=0.8) stay below it. After the defect starts, the raw signal gives a sustained warning on day 105 and the two smoothed signals on day 107, so the failure limit is reached 36 and 34 days later, respectively, as panel (*b*) shows. Smoothing therefore removes the false alarms at the price of about two days of warning. The cumulative Cesàro mean never reaches the alarm limit within 145 days, because the 80 healthy days keep pulling its average down, which gives the long memory discussed in Section 4.2 a concrete cost.

© 2026 Abnus | Open Access — CC BY 4.0 | abnus.co | DOI:10.52909/jti.v6i2.462

Whether two days of warning is a fair price for two fewer false alarms depends on the costs in Table 6, and the raw record should be kept next to the smoothed trend because a genuine impulsive fault would be attenuated in the same way as the startup spikes.

4.10 Case Studies on Public Run to Failure Data

Three public run to failure collections allow the framework to be tied to real equipment, although no results from them are reported here. The IMS bearing dataset from the University of Cincinnati was recorded on a rig in which several bearings ran under constant load and speed until failure (Lee et al., 2007), and such records contain a long healthy plateau followed by a late, accelerating rise in vibration energy. The NASA battery dataset records repeated charge and discharge cycles until capacity has faded by a stated amount (Saha & Goebel, 2007), and capacity falls slowly but not smoothly because rest periods can lift the measured value for a few cycles. The turbofan data contain simulated run to failure trajectories with multiple sensors and operating conditions (Saxena & Goebel, 2008), and a later dataset provides trajectories under real flight conditions (Arias Chao et al., 2021). The data problem each setting raises is sketched in Figure 13.

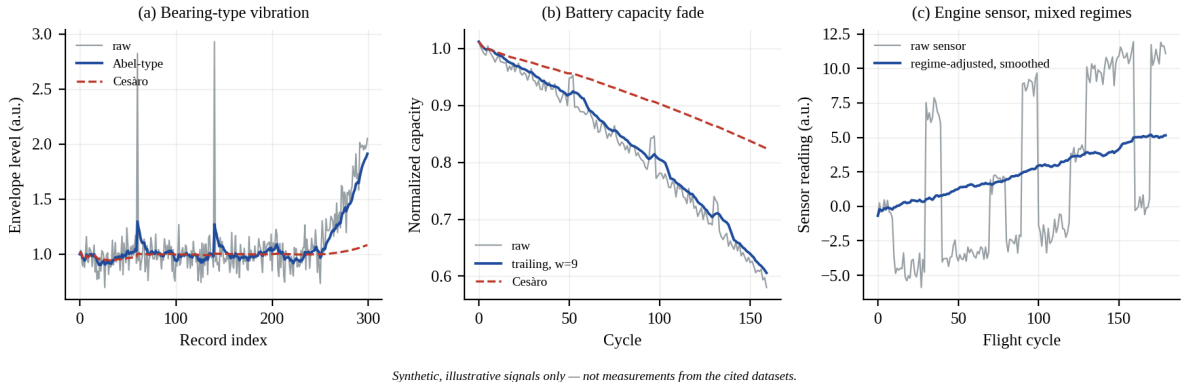


Figure 13. Three public data settings and the data problem each raises, showing (a) bearing type vibration with startup spikes and late degradation, (b) battery capacity fade with temporary recoveries, and (c) an engine sensor whose level jumps with the operating regime (signals are synthetic)

Figure 13 shows in panel (*a*) a bearing type vibration signal with isolated startup spikes and a late accelerating rise, where a short trailing or Abel type mean keeps the knee of the curve visible while the Cesàro mean is dominated by the long healthy history and reacts late. Panel (*b*) shows battery capacity fade with temporary recoveries, where a moderate trailing window removes the jumps while following the fade, whereas the Cesàro mean overstates remaining capacity as the fade accelerates, which is the risky direction for a safety related estimate. Panel (*c*) shows an engine sensor whose level jumps whenever the flight regime changes, so each reading should be normalized within its regime before a trailing or Abel type mean is applied. Together the panels show the same discipline across industries, namely matching operator memory to the way the signal ages, removing known nondegradation effects before averaging, and judging the choice by warning time, false alarms, and cost rather than by visual smoothness.

4.11 Discussion

The main contribution of summability in this framework is explicit control over how temporal observations are aggregated. Rather than treating smoothing as an undocumented default, the operator and its memory structure become testable design choices, with Cesàro averaging emphasizing accumulated history, finite window averaging imposing a clear memory horizon, and Abel type weighting making recency adjustable. This vocabulary connects mathematical properties to engineering behavior, consistent with the view that summability methods can regularize irregular sequences in engineering systems (Sahani, Sahani, Jha, & Mahato, 2026). Summability does not, however, infer an unrecorded maintenance intervention, repair informative censoring, correct a

miscalibrated sensor, or distinguish load change from damage without context, and a smoother signal does not automatically imply a better estimate of hazard or RUL. The defensible expectation is conditional, because smoothing is most likely to help when high frequency variation is mostly measurement noise and degradation evolves more slowly than the window, and least likely to help when failure precursors are impulsive or processes change abruptly. The workflow should therefore preserve parallel views of the signal, with raw data for transients, smoothed data for drift, robust features against spikes, and contextual features for normal operating changes (Barredo Arrieta et al., 2020).

5. Conclusions

Noisy industrial reliability data require more than a smoothing filter and more than a prediction score. A credible analysis must preserve event and censoring information, separate measurement artifacts from operational changes, model the relevant failure quantity, validate predictions on future or unseen assets, and translate uncertainty into a maintenance policy. Summability methods provide a transparent family of temporal aggregation operators that can be tested as one component of this pipeline. The Cesàro mean offers cumulative stabilization but retains long memory, finite window means offer bounded memory at the cost of a tunable lag, and Abel type weighting provides recency control. The generated illustrations show that these properties produce real trade offs, such as the slow recovery of the Cesàro mean after a regime shift and the exchange of false alarms for warning time in the pump example, and that none of the operators guarantees improved failure prediction. The central recommendation is to use summability as an explicit and auditable candidate transformation while retaining raw signals, context, and event metadata, and to judge it through survival aware metrics, calibration, warning lead time, and cost sensitivity.

Acknowledgement

The authors thank the Faculty of Science, Technology, and Engineering, Rajarshi Janak University, Janakpurdham, Nepal, for its academic support, and acknowledge the providers of the public datasets discussed in this study, including the NASA Prognostics Center of Excellence and the Center for Intelligent Maintenance Systems, University of Cincinnati.

Author Contributions

AS contributed to the conceptualization of the study, methodology, mathematical formulation, visualization, and the writing, review, and editing of the manuscript. PKN contributed to the conceptualization of the study, methodology, mathematical formulation, visualization, and the writing, review, and editing of the manuscript. SKS contributed to the conceptualization of the study, methodology, mathematical formulation, visualization, and the writing, review, and editing of the manuscript. All authors read and approved the final manuscript.

Conflict of Interest

The authors declare that there is no conflict of interest regarding the publication of this article. The study received no specific funding, and the authors have no financial, commercial, or personal relationships that could have influenced the work reported in this paper.

References

Arias Chao, M., Kulkarni, C., Goebel, K., & Fink, O. (2021). Aircraft engine run to failure dataset under real flight conditions for prognostics and diagnostics. *Data*, *6*(1). https://doi.org/10.3390/data6010005

Barredo Arrieta, A., Díaz-Rodríguez, N., Del Ser, J., Bennetot, A., Tabik, S., Barbado, A., Garcia, S., Gil-Lopez, S., Molina, D., Benjamins, R., Chatila, R., & Herrera, F. (2020). Explainable artificial intelligence (XAI): Concepts, taxonomies, opportunities and challenges toward responsible AI. *Information Fusion, 58, 82–115*. https://doi.org/10.1016/j.inffus.2019.12.012

Guidotti, D., Pandolfo, L., & Pulina, L. (2025). A systematic literature review of supervised machine learning techniques for predictive maintenance in Industry 4.0. *IEEE Access, 13, 102479–102504*. https://doi.org/10.1109/ACCESS.2025.3578686

Haixiang, G., Yijing, L., Shang, J., Mingyun, G., Yuanyue, H., & Bing, G. (2017). Learning from class imbalanced data: Review of methods and applications. *Expert Systems with Applications, 73, 220–239*. https://doi.org/10.1016/j.eswa.2016.12.035

Kapoor, S., & Narayanan, A. (2023). Leakage and the reproducibility crisis in machine learning based science. *Patterns*, *4*(9). https://doi.org/10.1016/j.patter.2023.100804

Kushwaha, J. K., Thakur, A. K., Sahani, S. K., & Suryawanshi, H. (2023). Existence and convergence of gamma matrices and their application to infinite series. *The Mathematical Education*, *57*(2), 17-30.

Lee, J., Qiu, H., Yu, G., Lin, J., & Rexnord Technical Services. (2007). *Bearing data set [Data set]*.

Lei, Y., Li, N., Guo, L., Li, N., Yan, T., & Lin, J. (2018). Machinery health prognostics: A systematic review from data acquisition to RUL prediction. *Mechanical Systems and Signal Processing, 104, 799–834*. https://doi.org/10.1016/j.ymssp.2017.11.016

Lei, Y., Yang, B., Jiang, X., Jia, F., Li, N., & Nandi, A. K. (2020). Applications of machine learning to machine fault diagnosis: A review and roadmap. *Mechanical Systems and Signal Processing, 138, Article 106587*. https://doi.org/10.1016/j.ymssp.2019.106587

Lu, J., Liu, A., Dong, F., Gu, F., Gama, J., & Zhang, G. (2019). Learning under concept drift: A review. *IEEE Transactions on Knowledge and Data Engineering*, *31*(12), 2346-2363. https://doi.org/10.1109/TKDE.2018.2876857

NIST/SEMATECH. (2012). Engineering statistics handbook, Chapter 8 Assessing product reliability. *National Institute of Standards and Technology*. Retrieved from https://www.itl.nist.gov/div898/handbook/apr/apr.htm

Njor, E., Hasanpour, M. A., Madsen, J., & Fafoutis, X. (2024). A holistic review of the TinyML stack for predictive maintenance. *IEEE Access, 12, 184861–184882*. https://doi.org/10.1109/ACCESS.2024.3512860

Pang, G., Shen, C., Cao, L., & van den Hengel, A. (2022). Deep learning for anomaly detection: A review. *ACM Computing Surveys*, *54*(2). https://doi.org/10.1145/3439950

Pokharel, J. K., Pahari, N. P., & Sahani, S. K. (2023). Critical analyzing on some new application of almost decreasing sequence to Legendre series associated with [B] sum. *Advances in Nonlinear Variational Inequalities*, *26*(2), 36-40. https://doi.org/10.52783/anvi.v26.253

Saha, B., & Goebel, K. (2007). Battery data set [Data set]. *NASA Ames Prognostics Center of Excellence*.

Sahani, S. K., & Das, G. (2023). Generalized almost matrix summability of Fourier series and its conjugate series. *Tuijin Jishu/Journal of Propulsion Technology*, *43*(3), 2635-2655.

Sahani, S. K., & Mishra, L. N. (2021). Degree of approximation of signals by Nörlund summability of derived Fourier series. *The Nepali Mathematical Sciences Report*, *38*(2), 13-19. https://doi.org/10.3126/nmsr.v38i2.42845

Sahani, S. K., & Mishra, V. N. (2020). A certain study on Nörlund summability of series. *Journal of Linear and Topological Algebra*, *9*(4), 311-321.

Sahani, S. K., Mishra, V. N., & Pahari, N. P. (2020). On the degree of approximation of functions by N means of their Fourier Laguerre series. *Nepal Journal of Mathematical Sciences, 1, 65–70*. https://doi.org/10.3126/njmathsci.v1i0.34164

Sahani, S. K., Mishra, V. N., & Rathour, L. (2022). On Nörlund summability of double Fourier series. *Open Journal of Mathematical Sciences*, *6*(1), 99-107. https://doi.org/10.30538/oms2022.0180

Sahani, S. K., Sahani, K., Jha, A., & Mahato, A. (2026). Regularization of divergent series via classical summability methods with applications to reliability and engineering systems. *International Journal of Prognostics and Health Management*, *17*(2). https://doi.org/10.36001/IJPHM.2026.v17i2.4750

Sahani, S. K., Thakur, A. K., & Dubey, A. (2022). Degree of approximation of conjugate of function belonging to (N, p, q) class by matrix summability means of conjugate Fourier series. *Mathematical Statistician and Engineering Applications*, *71*(4), 321-331.

Saxena, A., & Goebel, K. (2008). Turbofan engine degradation simulation data set [Data set]. *NASA Ames Prognostics Data Repository*.

Serradilla, O., Zugasti, E., Rodriguez, J., & Zurutuza, U. (2022). Deep learning models for predictive maintenance: A survey, comparison, challenges and prospects. *Applied Intelligence*, *52*(10), 10934-10964. https://doi.org/10.1007/s10489-021-03004-y

Severson, K. A., Attia, P. M., Jin, N., Perkins, N., Jiang, B., Yang, Z., Chen, M. H., Aykol, M., Herring, P. K., Fraggedakis, D., Bazant, M. Z., Harris, S. J., Chueh, W. C., & Braatz, R. D. (2019). Data driven prediction of battery cycle life before capacity degradation. *Nature Energy*, *4*(5), 383-391. https://doi.org/10.1038/s41560-019-0356-8

Syed, M. A. B., Hasan, M. R., Chowdhury, N. I., Rahman, M. H., & Ahmed, I. (2025). A systematic review of time series algorithms and analytics in predictive maintenance. *Decision Analytics Journal, 15, Article 100573*. https://doi.org/10.1016/j.dajour.2025.100573

Truong, C., Oudre, L., & Vayatis, N. (2020). Selective review of offline change point detection methods. *Signal Processing, 167, Article 107299*. https://doi.org/10.1016/j.sigpro.2019.107299

Wang, P., Li, Y., & Reddy, C. K. (2019). Machine learning for survival analysis: A survey. *ACM Computing Surveys*, *51*(6). https://doi.org/10.1145/3214306

Zhao, R., Yan, R., Chen, Z., Mao, K., Wang, P., & Gao, R. X. (2019). Deep learning and its applications to machine health monitoring. *Mechanical Systems and Signal Processing, 115, 213–237*. https://doi.org/10.1016/j.ymssp.2018.05.050

Zonta, T., da Costa, C. A., da Rosa Righi, R., de Lima, M. J., da Trindade, E. S., & Li, G. P. (2020). Predictive maintenance in the Industry 4.0: A systematic literature review. *Computers & Industrial Engineering, 150, Article 106889*. https://doi.org/10.1016/j.cie.2020.106889